ANTIMICROBIAL AGENTS AND CHEMOTHERAPY, May 2005, p. 2026–2034 Vol. 49, No. 5
0066-4804/05/$08.00+0 doi:10.1128/AAC.49.5.2026–2034.2005

Mechanistic Study of the Photodynamic Inactivation of *Candida albicans* by a Cationic Porphyrin

S. A. G. Lambrechts,[1] M. C. G. Aalders,[1]* and J. Van Marle[2]

Laser Center[1] and Department of Cell Biology and Histology,[2] Academic Medical Center, University of Amsterdam, Meibergdreef 9, 1105 AZ Amsterdam, The Netherlands

Received 28 July 2004/Returned for modification 31 October 2004/Accepted 12 January 2005

The growing resistance against antifungal agents has renewed the search for alternative treatment modalities, and antimicrobial photodynamic inactivation (PDI) is a potential candidate. The cationic porphyrin 5-phenyl-10,15,20-Tris(*N*-methyl-4-pyridyl)porphyrin chloride (TriP[4]) is a photosensitizer that in combination with light can inactivate bacteria, fungi, and viruses. For future improvement of the efficacy of PDI of clinically relevant fungi such as *Candida albicans*, we sought to understand the working mechanism by following the response of *C. albicans* exposed to PDI using fluorescence confocal microscopy and freeze-fracture electron microscopy. The following events were observed under dark conditions: TriP[4] binds to the cell envelope of *C. albicans*, and none or very little TriP[4] enters the cell. Upon illumination the cell membrane is damaged and eventually becomes permeable for TriP[4]. After lethal membrane damage, a massive influx of TriP[4] into the cell occurs. Only the vacuole membrane is resistant to PDI-induced damage once TriP[4] passes the plasma membrane. Increasing the incubation time of *C. albicans* with TriP[4] prior to illumination did not increase the influx of TriP[4] into the cell or the efficacy of PDI. After the replacement of 100% phosphate-buffered saline (PBS) by 10% PBS as the medium, *C. albicans* became permeable for TriP[4] during dark incubation and the efficacy of PDI increased dramatically. In conclusion, *C. albicans* can be successfully inactivated by the cationic porphyrin TriP[4], and the cytoplasmic membrane is the target organelle. TriP[4] influx occurred only after cell death.

Interest in the photodynamic inactivation (PDI) of yeasts was initially based on the role of the yeast as a model organism. They are easy to cultivate and can be used for research that is too complicated to be performed with higher cells. Yeasts such as *Saccharomyces cerevisiae* and *Kluyveromyces marxianus* have been used as model organisms to assess the cell damage induced by PDI in eukaryotic cells (14, 31, 40, 44).

The clinical application of PDI is called photodynamic therapy and is a treatment modality that is used for the treatment of certain superficial malignancies (10, 21). It employs visible light to activate a light-sensitive compound, the photosensitizer. The activated photosensitizer can subsequently react with molecules in its direct environment either by electron or hydrogen transfer, which leads to the production of radicals (type 1 reaction), or by energy transfer to oxygen, which generates the highly reactive singlet oxygen (type 2 reaction). Both pathways can lead to cell death.

Recently, the growing resistance against antifungal agents has renewed interest in the PDI of fungi (34). The focus is now mainly on the PDI of pathogenic or potentially pathogenic fungi like *Aspergillus fumigatus* (9), *Trichophyton rubrum* (36), and especially *Candida albicans* (3, 5, 15, 41), which is a common inhabitant of the mouth, throat, digestive tract, and skin. In hosts with a compromised immune system it can become pathogenic (8, 11). Oropharyngeal candidiasis is one of the most common opportunistic infections accompanying AIDS patients. Resistance of *C. albicans* against fluconazole, an antifungal agent frequently used by such patients, has begun to appear (34).

In the last decade, cationic porphyrins (2, 23, 24), phthalocyanines (26, 27, 37), and chlorins (12) have gained popularity as antimicrobial photosensitizers due to their abilities to inactivate both gram-positive and gram-negative bacteria. This has fueled the thought that these photosensitizers could be successfully applied as broadband antimicrobial agents. In order to optimize the PDI of microorganisms, knowledge of the underlying mechanisms is indispensable. However, in the majority of studies investigating the mechanisms of yeast PDI, the anionic hematoporphyrin and its derivatives (3, 39), the hydrophobic chloroaluminum phthalocyanine (29, 32) or the cationic thiazine dye toluidine blue (6, 13, 28, 30), are used as photosensitizers.

In a previous study we have observed that *C. albicans* could be successfully photoinactivated using the cationic porphyrin 5-phenyl-10,15,20-Tris(*N*-methyl-4-pyridyl)porphyrin chloride (TriP[4]) as a photosensitizer. However, the efficacy of PDI was reduced dramatically when albumin was present in the medium (20).

The purpose of this study was to increase our insight into the sequential steps by which *C. albicans* is photoinactivated using the cationic porphyrin TriP[4] as a photosensitizer. We employed fluorescence confocal microscopy to visualize the location in the cell of TriP[4] and freeze-fracture electron microscopy to study the integrity of the plasma membrane of *C. albicans* at various stages of the PDI process.

* Corresponding author. Mailing address: Laser Center K01-225-5, Academic Medical Center, Meibergdreef 9, 1105 AZ Amsterdam, The Netherlands. Phone: 31 (0)20 566 3829. Fax: 31 (0)20 697 5594. E-mail: M.C.Aalders@amc.uva.nl.

MATERIALS AND METHODS

Microorganisms. A *C. albicans* strain isolated from a burn wound from a patient was kindly provided by the Central Bacteriological Laboratory (Haarlem,

The Netherlands). *C. albicans* was grown aerobically overnight in 10 ml of brain heart infusion broth (Oxoid Ltd., Hampshire, United Kingdom) at 37°C, harvested after centrifugation at 3,000 rpm for 10 min, and washed twice with phosphate-buffered saline (PBS; pH 7.4).

Photosensitizer. A 1 mM (0.78 mg · ml^{-1}) stock solution of the photosensitizer TriP[4] (99% pure; Porphyrin Systems GbR, Lübeck, Germany) was prepared in PBS (pH 7.4) and stored at 4°C in the dark. The concentration of TriP[4] was checked by using the optical density (OD); 1 mM TriP[4] in methanol gives an OD of 1.58 at 424 nm in a 1-cm cuvette. Prior to use, the stock solution was allowed to warm to room temperature.

Light source. All illuminations were carried out with white light from a 500-W halogen lamp (PROmax-Vega, China). To avoid heating of the samples, the light was passed through a 1-cm-thick water filter. The fluence rate at the level of the microorganism samples was 30 mW · cm^{-2}, as measured with a power meter (Optilas; Ophir Optronics Ltd., Israel). During the illumination procedure, the temperature of the samples never exceeded 22°C. The temperature was measured at the cell level with a Fluke (Everett, WA) 52 K/J thermometer.

PDI studies. The *C. albicans* pellet was resuspended in 2 ml of PBS (pH 7.4) and was subsequently diluted 10-fold with PBS (pH 7.4) or with demineralized water, which resulted in a 10% PBS solution. The final cell concentration of the suspensions was 10^6 to 10^7 cells · ml^{-1}. The cell suspensions were incubated with 25 μM TriP[4] for 1, 15, or 30 min, after which 1-ml aliquots of the suspensions were transferred to polystyrene culture dishes with a diameter of 3 cm (Greiner; Greiner Bio-One International, Frickenhausen, Germany) and illuminated. To eliminate the effect of the TriP[4] in solution or loosely bound to the cell wall, we also performed PDI experiments with cells that, after a 30-min incubation with 25 μM Trip[4] in PBS, were washed twice with PBS prior to illumination.

Cell survival was determined by a modified version of the Miles and Misra (25) method. For this, the suspensions were serially 10-fold diluted with PBS. Then, drops of 10 μl of each dilution were applied onto Iso-Sensitest agar (Oxoid Ltd., Hampshire, United Kingdom) fivefold and incubated at 37°C under aerobic conditions. After 48 h the number of CFU was counted. Survival was expressed as a percentage relative to that for a control sample containing no photosensitizer taken at the beginning of each experiment, prior to illumination. Survival was also determined for samples after illumination in the absence of photosensitizer and for samples after incubation with the photosensitizer in the dark. Under the illumination conditions described in this article, TriP[4] is known to remain stable (35).

Fluorescence emission and absorption spectra. To assess the optimal excitation and detection wavelengths for the fluorescence confocal microscopy experiments, the absorption and fluorescence emission spectra of TriP[4] were taken. Solutions of 1 and 10 μM TriP[4] were prepared in PBS (pH 7.4) and ethanol; the absorption spectra were recorded at room temperature by using a spectrophotometer (Ultrospec 2000; Pharmacia Biotech Ltd., Cambridge, United Kingdom). Fluorescence emission spectra were recorded at room temperature with an excitation wavelength of 543 nm, using a spectrofluorometer (FP-750; Jasco Benelux B.V., Maarssen, The Netherlands). In addition, a fluorescence emission spectrum of a *C. albicans* suspension in PBS that had received a light dose of 27 J · cm^{-2} was taken after just 1 min of incubation with 25 μM TriP[4]. Before the fluorescence emission spectrum was taken, the treated cell suspension was washed once with PBS to remove the TriP[4] from the medium.

Fluorescence labeling. For the intracellular localization of TriP[4], the cells were labeled with fluorescence markers after PDI, using a light/photosensitizer dose of 9 J · cm^{-2}/25 μM TriP[4]. The nuclei were labeled with a DNA-specific fluorescent dye, Hoechst 33342 (Sigma-Aldrich) (7), at a concentration of 1 μg · ml^{-1} for 10 min in PBS (pH 7.4) at room temperature. The lumen of the vacuole was labeled with the specific fluorescent dye CellTracker Blue CMAC (Molecular Probes, Leiden, The Netherlands) (18, 38) at a concentration of 100 μM for 10 min in PBS (pH 7.4) at room temperature. The labeled cells were imaged by confocal fluorescence microscopy.

After treatment, the *C. albicans* cells were harvested by centrifugation at 3,000 rpm for 10 min. A Leica SP2 confocal microscope was used for imaging. On the basis of the absorption spectra (Fig. 1A) of TriP[4], the 543-nm line of an HeNe laser was used for excitation of TriP[4]. On the basis of the fluorescence spectra of TriP[4] (Fig. 1B), the detection bandwidth used was 620 to 750 nm.

For Hoechst 33342 staining, excitation was performed with the 351-nm line of an argon ion laser, and the detection bandwidth used was 410 to 460 nm. Detection of CellTracker Blue CMAC was performed with excitation at 351 nm and detection between 450 and 490 nm.

Images were acquired in an eight-bit format. An HCL PL APO 63 × 1.32 oil immersion objective was used with a zoom factor of 4, which resulted in a pixel size of 116 nm · 116 nm. The pinhole was fixed at a diameter of 1 Airy disk, which corresponded to an axial resolution of approximately 0.5 μm. Simultaneously with the confocal fluorescence images, transmitted light differential interference contrast (DIC) images were collected. Merging of the images was done with dedicated Leica software. To demonstrate the effects of PDI, equatorial sections of the yeasts are presented with corresponding DIC transmitted light images.

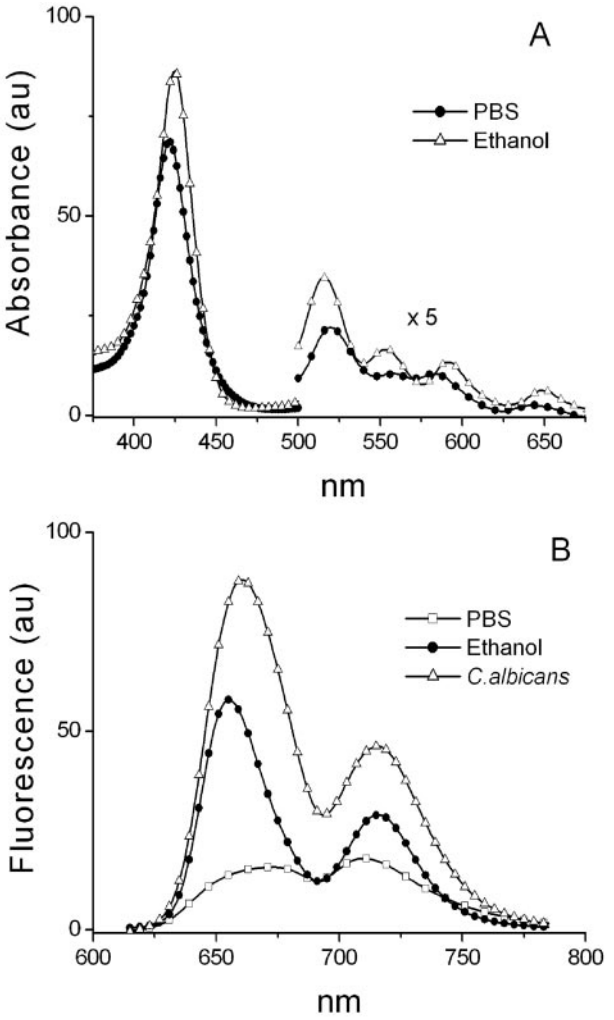

FIG. 1. (A) Absorption spectra of 10 μM TriP[4] in ethanol (△) and PBS (●); (B) fluorescence spectra of 1 μM TriP[4] in ethanol (●) and PBS (□) and of a *C. albicans* suspension in PBS (△) after PDI treatment with 25 μM TriP[4]/27 J · cm^{-2} and one wash with PBS after illumination. Fluence rate, 30 mW · cm^{-2}; au, arbitrary units.

Freeze-fracture electron microscopy. Specimens were fixed in McDowall's fixative for 24 h, washed in buffer, and cryoprotected with 2.3 M sucrose in 0.1 M phosphate buffer (pH 7.4). The specimens were frozen in liquid ethane (100 K) and fractured in a BAF300 instrument at a temperature of 150 K and a vacuum better than 4 × 10^{-5} Pa. Platinum (2 nm) was deposited at an angle of 45°, and 20-nm-diameter carbon was deposited at an angle of 90° to strengthen the replica. The replicas were cleansed with common household bleach overnight, washed with distilled water, and collected on a bare 300-mesh copper grid. The replicas were studied with a Philips EM420 electron microscope operated at 100 kV.

Statistics. Survival values are expressed as means ± standard deviations. Differences between means of multiple groups were analyzed by a Student's *t* test. Statistical significance was assumed at a *P* value of <0.05.

RESULTS

The results of experiments discussed below are summarized in Table 1. Fluorescence emission and absorption spectra. The absorption spectrum of 10 μM TriP[4] in ethanol consisted of

TABLE 1. Results of PDI experiments[a]

Light dose ($J \cdot cm^{-2}$)	% Survival (SD)	TriP[4] fluorescence pattern	Electron microscopy	
			e face	p face
0	70.3 (47.6)	Peripheral circular		
1.8	46.2 (46.2)	Peripheral circular	Fewer IMPs, rectangular areas without structure, phase separation	Patches without structure
5.4	0.20 (0.09)	Peripheral circular or cytoplasmic without a vacuole	Fewer IMPs, rectangular areas without structure are larger, phase separation	Fewer IMPs, phase separation, more patches without structure, blebbing
12.6	No survival detectable	Cytoplasmic without a vacuole	No IMPs, rectangular areas have merged	Less IMPs, phase separation, more patches without structure, blebbing

[a] The incubation time was 1 min. The results are for confocal and electron microscopy images of *C. albicans* cells diluted in PBS and illuminated in the presence of 25 μM TriP[4]. The fluence rate was 30 $mW \cdot cm^{-2}$.

a Soret band at 426 nm and Q bands at 518, 557, 594, and 652 nm. The absorption spectrum of 10 μM TriP[4] in PBS showed a Soret band at 423 nm and Q bands at 523, 560, 588, and 647 nm (Fig. 1A). The fluorescence spectrum of 1 μM TriP[4] suspended in PBS showed two coalesced weak emission peaks, Q (0,0) at 673 nm and Q (0,1) at 710 nm (Fig. 1B). In ethanol, the fluorescence spectrum of 1 μM TriP[4] showed two well-resolved emission peaks: Q (0,0) at 655 nm and Q (0,1) at 716 nm. The absorption and emission bands agree with data from the literature on (*N*-methyl-4-pyridyl)porphyrins (17, 22, 42). The fluorescence signal was stronger when ethanol was used as the solvent than when PBS was used as the solvent. The fluorescence emission spectrum of a *C. albicans* suspension that had received a light/photosensitizer dose of 27 $J \cdot cm^{-2}$/25 μM TriP[4] showed emission peaks at 661 and 715 nm (Fig. 1B) which were not observed in the spectrum of a control sample of *C. albicans* without TriP[4] (data not shown).

PDI studies. Figure 2A shows that *C. albicans* suspended in PBS could be successfully inactivated by 25 μM TriP[4] after just 1 min of incubation. After a light dose of 5.4 $J \cdot cm^{-2}$, a significant ($P < 0.01$) reduction in viability count was observed; and after a light dose of 12.6 $J \cdot cm^{-2}$ a 5.6-$\log_{10}$-unit reduction in viability count ($P < 0.01$) was obtained. Prolongation of the incubation time from 1 min to 30 min did not affect the survival of the cells. Furthermore, no killing was observed after TriP[4] incubation in the dark or illumination in the absence of TriP[4] (data not shown). Washing of the *C. albicans* cells after 30 min of incubation with 25 μM prior to illumination inhibited the PDI completely.

When *C. albicans* was suspended in a 10% PBS buffer with 25 μM TriP[4], a 3-$\log_{10}$-unit reduction in the viability count was obtained after a light dose of 0.9 $J \cdot cm^{-2}$ (Fig. 2B). No viable cells were found after a light dose of 1.8 $J \cdot cm^{-2}$. There was a significant reduction in viability count of 1 $\log_{10}$ unit after 7 min of incubation in 10% PBS with 25 μM TriP[4] in the dark ($P = 0.01$). Illumination in the absence of TriP[4] had no effect on the survival of *C. albicans*.

Fluorescence confocal microscopy. Figures 3 and 4 show the confocal fluorescence microscopy images of equatorial optical sections (left) and the corresponding DIC images (right) of *C. albicans* cells. Figure 3A shows *C. albicans* cells after incubation with 25 μM TriP[4] in PBS for 15 min in the dark. A longer incubation period of 30 min resulted in similar fluorescence patterns (data not shown). Circles of TriP[4] fluorescence were observed in the periphery of the cell, while no TriP[4] fluorescence was detected inside the cell. After an incubation time of 1 min, the same peripheral circular fluorescence patterns could be observed by wide-field fluorescence microscopy (data not shown), but this signal was too weak to be detected by confocal fluorescence microscopy. The fluores-

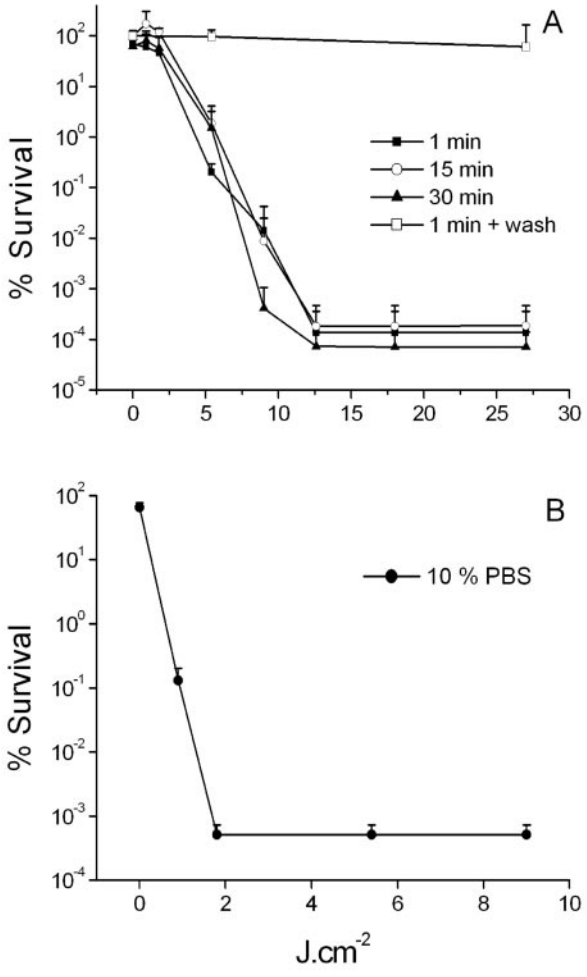

FIG. 2. (A) Photodynamic inactivation of *C. albicans* suspended in PBS with 25 μM TriP[4] with incubation times of 1, (■), 15 (○), and 30 (▲) min. Photodynamic inactivation of *C. albicans* incubated in PBS with 25 μM TriP[4] for 30 min and washed twice with PBS prior to illumination (□). Fluence rate, 30 $mW \cdot cm^{-2}$. Each point is the mean of three experiments ± standard deviation. (B) Photodynamic inactivation of *C. albicans* suspended in 10% PBS with 25 μM TriP[4] with an incubation time of 1 min (●). Fluence rate, 30 $mW \cdot cm^{-2}$. Each point is the mean of three experiments ± standard deviation.

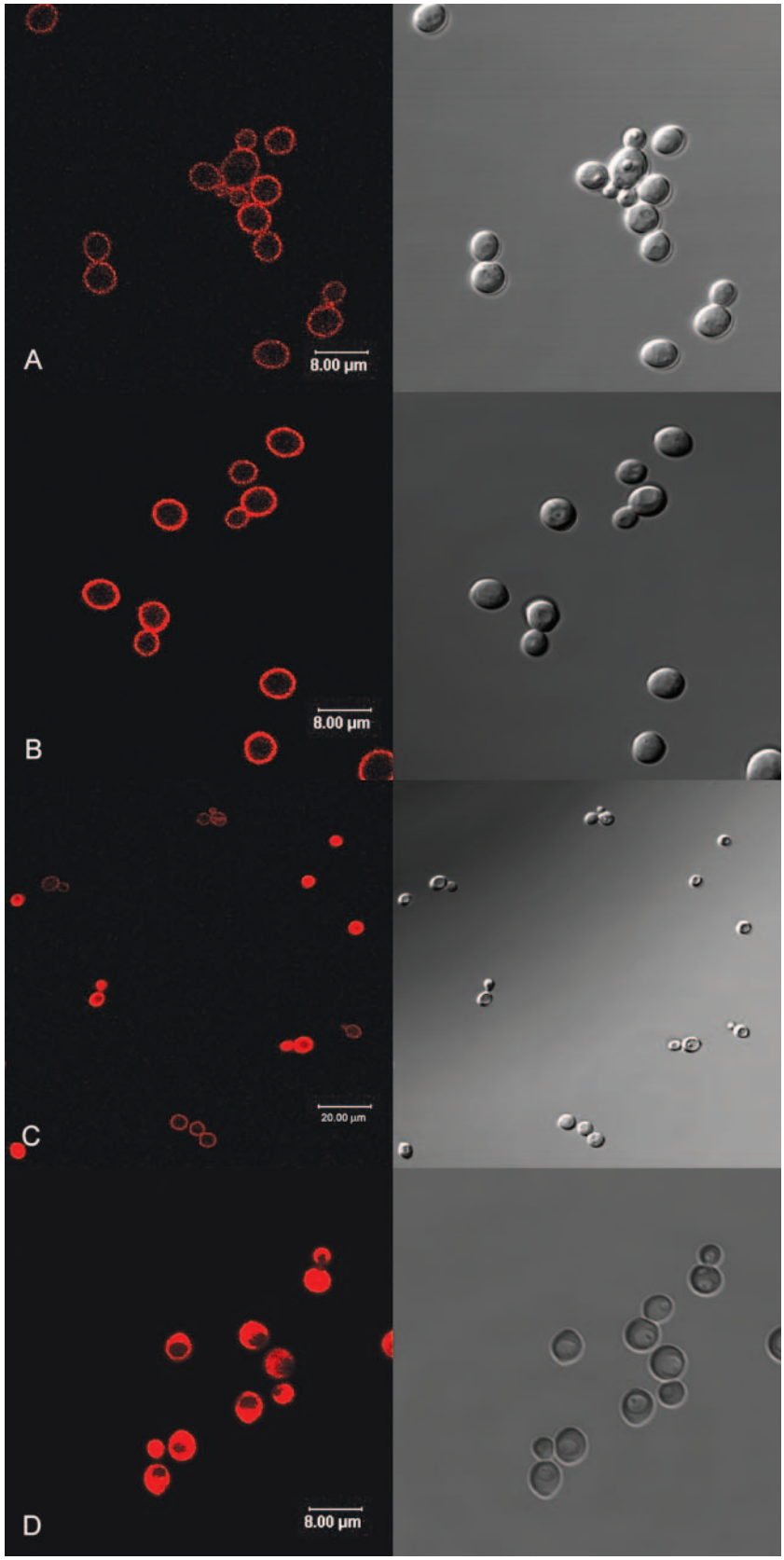

FIG. 3. Confocal fluorescence microscopy images (left) and the corresponding DIC images (right) of *C. albicans* cells in PBS. Dark incubation with 25 μM TriP[4] for 15 min (A). Illumination in the presence of 25 μM TriP[4] with light doses of 0.9 (B), 5.4 (C), and 12.6 (D) J · cm^{-2}. Fluence rate, 30 mW · cm^{-2}.

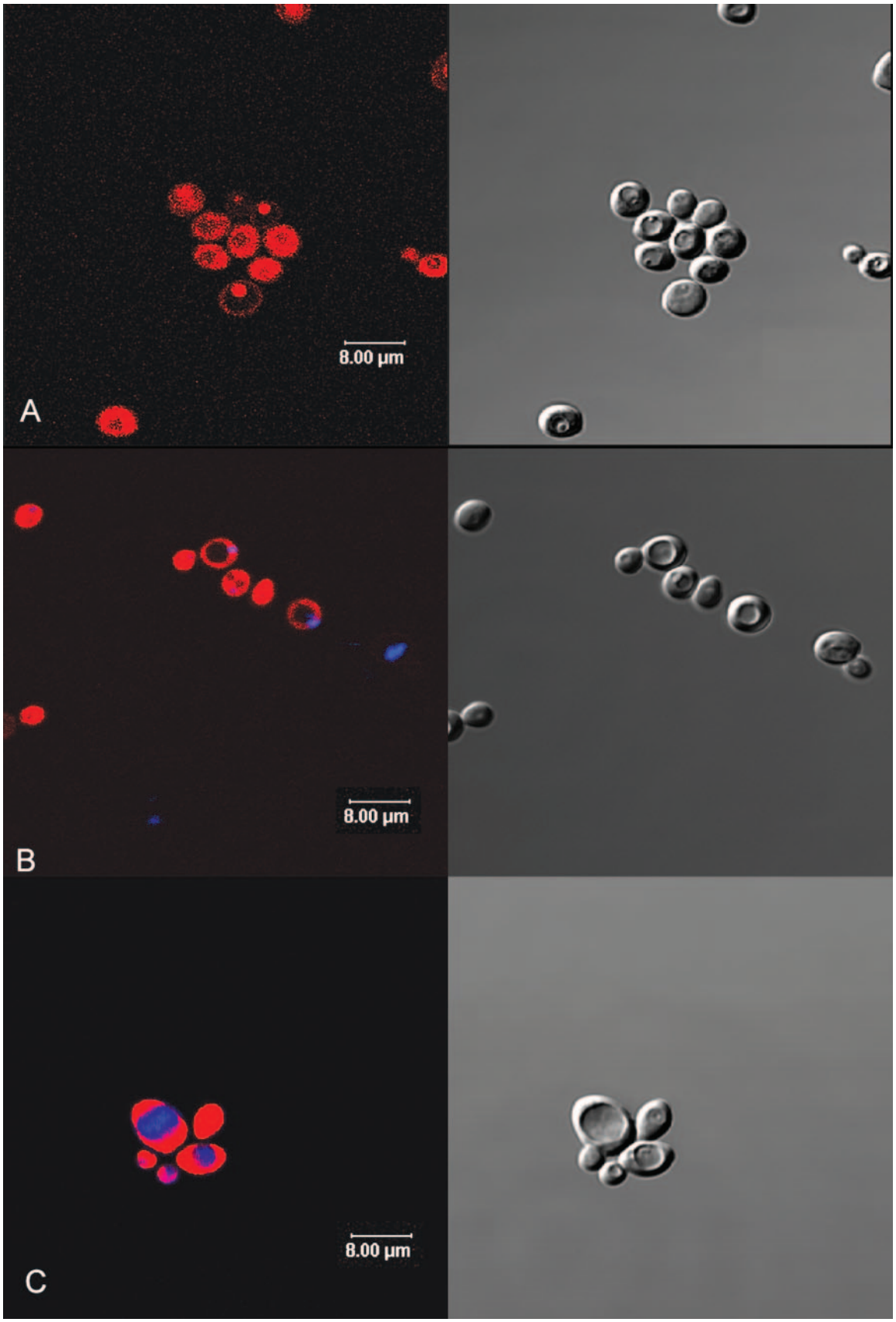

FIG. 4. Confocal fluorescence microscopy images (left) and the corresponding DIC images (right) of *C. albicans* cells. Dark incubation with 25 µM TriP[4] in 10% PBS for 30 min (A) and double labeling with the DNA dye Hoechst 33342 (blue) after illumination with 9 J · cm^{-2} in the presence of 25 µM TriP[4] (red) in PBS (B). Double labeling with the vacuole dye CellTracker Blue CMAC (blue) after illumination with 9 J · cm^{-2} in the presence of 25 µM TriP[4] (red) in PBS (C). Fluence rate, 30 mW · cm^{-2}.

cence patterns changed dramatically upon illumination. Figure 3B to D shows the fluorescence confocal microscopy images of *C. albicans* taken after different light doses in the presence of 25 μM TriP[4] suspended in PBS. Peripheral circles of TriP[4] fluorescence were observed up to 1.8 J · cm^{-2} (Fig. 3B). After a light dose of 5.4 J · cm^{-2} (Fig. 3C), the peripheral circles were observed in some cells, but other cells showed either no fluorescence at all or strong fluorescence in the entire cell except in a circular organelle. After a light dose of 9 J · cm^{-2}, the peripheral circular fluorescence patterns had disappeared and all cells showed complete TriP[4] fluorescence except in the circular organelle (data not shown). An increase in the light dose to 27 J · cm^{-2} did not induce additional effects, with the exception that some cells started to show TriP[4] fluorescence in the entire cell.

Incubation of *C. albicans* with 25 μM TriP[4] in 10% PBS for 30 min in the dark resulted in an ambiguous distribution of TriP[4] fluorescence (Fig. 4A). Some cells showed complete fluorescence, with the exception of one large circular organelle. Other cells showed no fluorescence in the cytoplasmic area, but some specific organelles and the cell envelope did show TriP[4] fluorescence. These distribution patterns were already observed after just 1 min of incubation in the dark.

Figure 4B shows *C. albicans* cells that were stained with the nuclear stain Hoechst after a light/photosensitizer dose of 9 J · cm^{-2}/25 μM TriP[4] in PBS. Blue depicts the nucleus, and red represents Trip[4]. TriP[4] entered the nucleus during PDI treatment. Figure 4C shows *C. albicans* cells that were stained with the vacuole stain CMAC Blue CellTracker after the same light/photosensitizer dose. In these images blue depicts CMAC Blue CellTracker and red represents Trip[4]. TriP[4] did not enter the vacuole during PDI treatment.

Freeze-fracture electron microscopy. Control *C. albicans* cells that received neither TriP[4] nor light presented p (protoplasmic) faces with numerous intermembrane proteins (IMPs) and troughs, i.e., invaginations of the plasma membrane into the cytoplasm (Fig. 5A). The e (extracellular) faces presented a membrane architecture with a few IMPs and structures complementary to the troughs on the p face (Fig. 5A, inset). *C. albicans* cells that had received a light/photosensitizer dose of 1.8 J · cm^{-2}/25 μM TriP[4] showed marked changes in the membrane architecture in comparison to that for the control. Changes on the p face itself were not observed, but large parts that were still attached to the p face showed a smooth fracture plane without IMPs (Fig. 5B). Since these fractures planes were higher than the p face of the yeast, they must have broken through the cell wall close to the outer extracellular face of the cell. Often, these smooth fracture planes showed a crystal-like appearance. Changes of the e face were pronounced, and smooth deeper fracture planes which seemed to run close to the outside of the plasma membrane through the cell wall were encountered (Fig. 5C); large parts had a fragmented rectangular appearance indicative of phase separation, with IMPs in between (Fig. 5D). At locations where the surface showed a normal structure, fewer IMPs were present compared to the numbers present in the control cells. After a light dose of 5.4 J · cm^{-2} the p face also became affected (Fig. 5E), showing clustering of IMPs in strings, which is representative of phase separation. The number of membrane folds in the p face increased, and broken yeasts and patches of increased numbers and sizes without structure appeared more often. The rectangular areas in the e face were larger (data not shown). After a light dose of 12.6 J · cm^{-2}, the phenomena described above were observed again, as did numerous cross-fractured cells, which is indicative of totally disintegrated membranes. In the p face (Fig. 5E, inset), there was a decrease in the number of IMPs. The membrane folds increased in number, and blebbing had become apparent.

DISCUSSION

Our results demonstrate that *C. albicans* can be successfully inactivated by the cationic porphyrin TriP[4] and that the cytoplasmic membrane is the target organelle. The confocal fluorescence microscopy images demonstrated that during incubation in PBS in the dark, TriP[4] did not enter or very slowly entered the cell, resulting in weak peripheral fluorescence patterns (Fig. 3A). This explains why a prolonged incubation time did not did not lead to an increase in TriP[4] uptake and subsequent PDI. Washing of the cells prior to illumination totally inhibited PDI, which is indicative of a weak binding of TriP [4] to the cell envelope. The fluorescence confocal images also show us that the cells had died before the massive influx of TriP[4] into the cell. After a light dose of 5.4 J · cm^{-2}, 99.8% of the cells were photoinactivated, even though only a small fraction of the cells showed fluorescence in the interior of the cell (Table 1; Fig. 3B). This indicates that damage to the cell membrane is enough for the PDI of *C. albicans* by TriP[4]. The large circular organelle that did not show any TriP[4] fluorescence during PDI (Table 1; Fig. 3B) was identified as the yeast vacuole (Fig. 4) (18, 38). Prolongation of illumination after cell death results in complete TriP[4] fluorescence. The nucleus was not able to exclude TriP[4] (Fig. 4).

The freeze-fracture images of the plasma membrane of *C. albicans* provided detailed information about the PDI-induced plasma membrane damage. The results clearly show that the damage progresses from the outside of the cytoplasmic membrane inward. This is illustrated by the onset of substantial damage in the e face after a light dose of 1.8 J · cm^{-2}, while the p face remained intact, except for some patches without a substantial structure. We think that these patches are the external surface of the plasma membrane. When a cell is freeze fractured, the breaking surface occurs along the line of least resistance, which is usually the hydrophobic middle of lipid bilayers (1). So, when the cell breaks over the external surface of the lipid bilayer, a loss of hydrophobicity in the center of the lipid bilayer is implied. Phase separation was already observed in both the e and the p faces of the PDI-treated yeast cells at an early stage in the PDI treatment. Blebbing is a known metabolic effect which occurs during cell death, and in this case it occurred when TriP[4] had entered the yeast after it had lost its viability (Table 1).

Our observations are very similar to those obtained for the PDI of *K. maxianus* with toluidine blue (30, 31) and the PDI of *C. albicans* with hematoporphyrin (3, 4). In both cases it was concluded that the plasma membrane became permeable during PDI, but the cell inactivation was attributed to more subtle forms of membrane damage, followed by damage to intracellular targets. The yeast vacuole was found to be resistant to toluidine blue-mediated PDI (30).

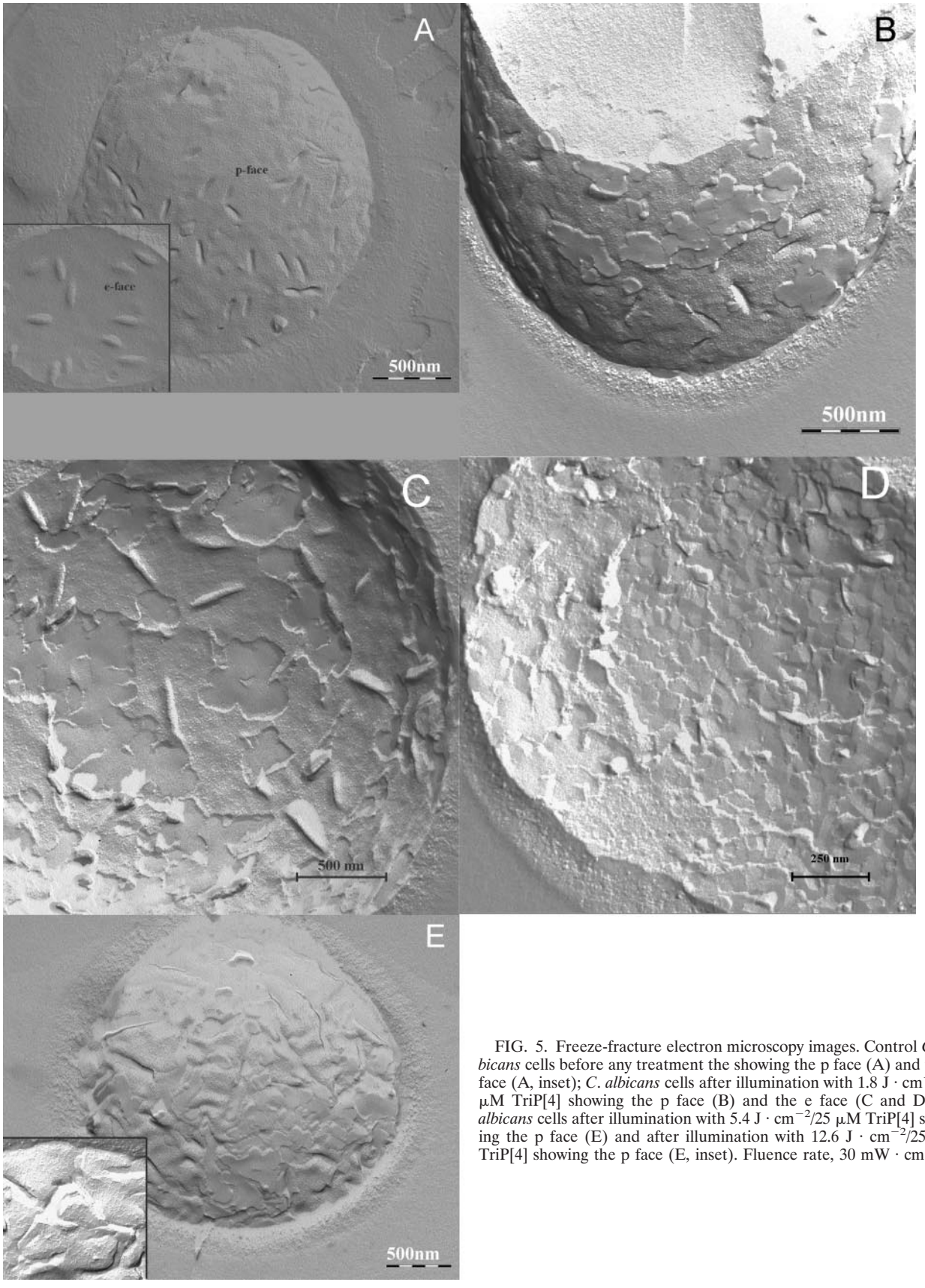

FIG. 5. Freeze-fracture electron microscopy images. Control *C. albicans* cells before any treatment the showing the p face (A) and the e face (A, inset); *C. albicans* cells after illumination with 1.8 J · cm^{-2}/25 μM TriP[4] showing the p face (B) and the e face (C and D); *C. albicans* cells after illumination with 5.4 J · cm^{-2}/25 μM TriP[4] showing the p face (E) and after illumination with 12.6 J · cm^{-2}/25 μM TriP[4] showing the p face (E, inset). Fluence rate, 30 mW · cm^{-2}.

In 10% PBS, *C. albicans* was more susceptible to PDI than it was in 100% PBS (Fig. 2B). This could be due to a lower ionic strength or could be due to a specific component in the buffer. We recently reported on the dependence of TriP[4]-mediated bacterial PDI on the ionic strength of the medium (19). Confocal fluorescence microscopy images taken after incubation of *C. albicans* with 25 μM TriP[4] suspended in the 10% PBS buffer in the dark showed that TriP[4] entered the cell (Fig. 4). This explains the moderate toxicity of TriP[4] under these conditions in the dark. The increased sensitivity of *C. albicans* to PDI in the 10% PBS buffer could be attributed to the increased permeability of the yeast membrane to TriP[4]. It should be taken into account that *C. albicans* is more vulnerable in diluted PBS than in 100% PBS due to the osmotic stress.

The fluorescence spectra (Fig. 1B) demonstrate that it is possible to observe the presence of TriP[4] in *C. albicans* without washing the cells before imaging, since the TriP[4] fluorescence signal in the hydrophilic PBS is much weaker than that in the more hydrophobic ethanol. The fluorescence behavior of TriP[4] is very similar to that of Tetrakis(*N*-methyl-4-pyridyl)porphyrin (TetraP[4]), and contradicting theories have been presented and withdrawn to explain the behavior (16, 17, 19, 33). To our knowledge, the only theory explaining the fluorescence behavior of TetraP[4] is currently offered by Vergeldt et al. (42). They hypothesized that the weak fluorescence signal of TetraP[4] and the lack of well-defined peaks in aqueous solutions is due to the mixing of the first excited electronic singlet state with a charge transfer state lying close by. The degree of mixing of the two states is partly determined by the solvent polarity; a lower dielectric constant of the solvent leads to a reduction in electronic coupling of the two states. Ethanol has a lower dielectric constant than water, 25.3 and 80.1 (at 293.2 K), respectively (43), and this explains why the Q (0,0) and Q (0,1) fluorescence bands are better resolved in ethanol than in PBS (Fig. 1B). Furthermore, Vergeldt et al. (42) observed that the adsorption of TetraP[4] to traces of solid material present in water also results in the resolved fluorescence spectrum, as observed in methanol. They conclude that no aggregation occurs below 10^{-3} μM in water.

The fluorescence spectrum shown in Fig. 1 of a suspension of *C. albicans* cells that had received a light/photosensitizer dose of 27 J · cm^{-2}/25 μM TriP[4] and that was subsequently washed with PBS to remove the TriP[4] from the suspension medium resembles the spectrum of 1 μM TriP[4] in ethanol. We think that this is due to both mechanisms mentioned by Vergeldt et al. (42).

In conclusion, *C. albicans* can be successfully inactivated by the cationic porphyrin TriP[4], and the cytoplasmic membrane is the target organelle. The electron microscopy images clearly show that the induced damage proceeds from the outer leaflet of the cytoplasmic membrane to the inner leaflet. The confocal fluorescence images showed that a massive influx of TriP[4] occurred after cell death.

REFERENCES

1. **Alberts, B., D. Bray, J. Lewis, M. Raff, K. Roberts, and J. D. Watson.** 1989. Molecular biology of the cell. Garland Publishing, Inc., New York, N.Y.
2. **Ashkenazi, H., Y. Nitzan, and D. Gal.** 2003. Photodynamic effects of antioxidant substituted porphyrin photosensitizers on gram-positive and -negative bacteria. Photochem. Photobiol. **77:**186–191.
3. **Bertoloni, G., E. Reddi, M. Gatta, C. Burlini, and G. Jori.** 1989. Factors influencing the haematoporphyrin-sensitized photoinactivation of Candida albicans. J. Gen. Microbiol. **135:**957–966.
4. **Bertoloni, G., F. Zambotto, L. Conventi, E. Reddi, and G. Jori.** 1987. Role of specific cellular targets in the hematoporphyrin-sensitized photoinactivation of microbial cells. Photochem. Photobiol. **46:**695–698.
5. **Bliss, J. M., C. E. Bigelow, T. H. Foster, and C. G. Haidaris.** 2004. Susceptibility of *Candida* species to photodynamic effects of photofrin. Antimicrob. Agents Chemother. **48:**2000–2006.
6. **Böcking, T., K. D. Barrow, A. G. Netting, T. C. Chilcott, H. G. Coster, and M. Hofer.** 2000. Effects of singlet oxygen on membrane sterols in the yeast Saccharomyces cerevisiae. Eur. J. Biochem. **267:**1607–1618.
7. **Ding, D. Q., Y. Chikashige, T. Haraguchi, and Y. Hiraoka.** 1998. Oscillatory nuclear movement in fission yeast meiotic prophase is driven by astral microtubules, as revealed by continuous observation of chromosomes and microtubules in living cells. J. Cell Sci. **111**(Pt 6)**:**701–712.
8. **Fridkin, S. K., and W. R. Jarvis.** 1996. Epidemiology of nosocomial fungal infections. Clin. Microbiol. Rev. **9:**499–511.
9. **Friedberg, J. S., C. Skema, E. D. Baum, J. Burdick, S. A. Vinogradov, D. F. Wilson, A. D. Horan, and I. Nachamkin.** 2001. In vitro effects of photodynamic therapy on Aspergillus fumigatus. J. Antimicrob. Chemother. **48:**105–107.
10. **Fritsch, C., G. Goerz, and T. Ruzicka.** 1998. Photodynamic therapy in dermatology. Arch. Dermatol. **134:**207–214.
11. **Garber, G.** 2001. An overview of fungal infections. Drugs **61**(Suppl. 1)**:**1–12.
12. **Hamblin, M. R., D. A. O'Donnell, N. Murthy, K. Rajagopalan, N. Michaud, M. E. Sherwood, and T. Hasan.** 2002. Polycationic photosensitizer conjugates: effects of chain length and Gram classification on the photodynamic inactivation of bacteria. J. Antimicrob. Chemother. **49:**941–951.
13. **Ito, T.** 1977. Toluidine blue: the mode of photodynamic action in yeast cells. Photochem. Photobiol. **25:**47–53.
14. **Ito, T.** 1981. Photodynamic action of hematoporphyrin on yeast cells—a kinetic approach. Photochem. Photobiol. **34:**521–524.
15. **Jackson, Z., S. Meghji, A. MacRobert, B. Henderson, and M. Wilson.** 1999. Killing of the yeast and hyphal forms of Candida albicans using a light-activated antimicrobial agent. Lasers Med. Sci. **14:**150–157.
16. **Kano, K., H. Minamizono, T. Kitae, and S. Negi.** 1997. Self-aggregation of cationic porphyrins in water. Can pi-pi stacking interaction overcome electrostatic repulsive force? J. Physical Chem. A **101:**6118–6124.
17. **Kano, K., T. Nakajima, M. Takei, and S. Hashimoto.** 1987. Self aggregation of cationic porphyrin in water. Chem. Soc. Jpn. **60:**1281–1287.
18. **Kohlwein, S. D.** 2000. The beauty of the yeast: live cell microscopy at the limits of optical resolution. Microsc. Res. Tech. **51:**511–529.
19. **Lambrechts, S. A. G., M. C. G. Aalders, D. H. Langeveld-Klerks, Y. Khayali, and J. W. M. Lagerberg.** 2003. Effect of monovalent and divalent cations on the photoinactivation of bacteria with meso-substituted cationic porphyrins. Photochem. Photobiol. **79:**297–302.
20. **Lambrechts, S. A. G., M. C. G. Aalders, F. D. Verbraak, J. W. Lagerberg, J. Dankert, and J. J. Schuitmaker.** 2005. Effect of albumin on the photoinactivation of microorganisms by a cationic porphyrin. J. Photochem. Photobiol. B Biol. **79:**51–57.
21. **Lopez, R. F., N. Lange, R. Guy, and M. V. Bentley.** 2004. Photodynamic therapy of skin cancer: controlled drug delivery of 5-ALA and its esters. Adv. Drug Deliv. Rev. **56:**77–94.
22. **Makarska, M., S. Radzki, and J. Legendziewicz.** 2002. Spectroscopic characterization of the water-soluble cationic porphyrins and their complexes with Cu(II) in various solvents. J. Alloys Compounds **341:**233–238.
23. **Merchat, M., G. Bertolini, P. Giacomini, A. Villanueva, and G. Jori.** 1996. Meso-substituted cationic porphyrins as efficient photosensitizers of gram-positive and gram-negative bacteria. J. Photochem. Photobiol. **32:**153–157.
24. **Merchat, M., J. D. Spikes, G. Bertoloni, and G. Jori.** 1996. Studies on the mechanism of bacteria photosensitization by meso-substituted cationic porphyrins. J. Photochem. Photobiol. **35:**149–157.
25. **Miles, A. A., and S. S. Misra.** 1938. The estimation of the bactericidal power of the blood. J. Hyg. **38:**732–749.
26. **Minnock, A., D. I. Vernon, J. Schofield, J. Griffiths, J. H. Parish, and S. B. Brown.** 1996. Photoinactivation of bacteria. Use of a cationic water-soluble zinc phthalocyanine to photoinactivate both gram-negative and gram-positive bacteria. J. Photochem. Photobiol. **32:**159–164.
27. **Minnock, A., D. I. Vernon, J. Schofield, J. Griffiths, J. H. Parish, and S. B. Brown.** 2000. Mechanism of uptake of a cationic water-soluble pyridinium zinc phthalocyanine across the outer membrane of *Escherichia coli*. Antimicrob. Agents Chemother. **44:**522–527.
28. **Oldham, T. C., and D. Phillips.** 1999. Flash photolysis of sensitizers in microbes. J. Physical Chem. B **103:**9333–9349.
29. **Paardekooper, M., A. W. De Bruijne, A. E. Van Gompel, R. A. Verhage, D. Averbeck, T. M. Dubbelman, and P. J. Van den Broek.** 1997. Single strand breaks and mutagenesis in yeast induced by photodynamic treatment with chloroaluminum phthalocyanine. J. Photochem. Photobiol. **40:**132–140.
30. **Paardekooper, M., A. W. De Bruijne, J. Van Steveninck, and P. J. Van den Broek.** 1995. Intracellular damage in yeast cells caused by photodynamic treatment with toluidine blue. Photochem. Photobiol. **61:**84–89.
31. **Paardekooper, M., P. J. Van den Broek, A. W. De Bruijne, J. G. Elferink,**

T. M. Dubbelman, and J. Van Steveninck. 1992. Photodynamic treatment of yeast cells with the dye toluidine blue: all-or-none loss of plasma membrane barrier properties. Biochim. Biophys. Acta **1108:**86–90.
32. **Paardekooper, M., A. E. Van Gompel, J. Van Steveninck, and P. J. Van den Broek.** 1995. The effect of photodynamic treatment of yeast with the sensitizer chloroaluminum phthalocyanine on various cellular parameters. Photochem. Photobiol. **62:**561–567.
33. **Reddi, E., M. Ceccon, G. Valduga, G. Jori, J. C. Bommer, F. Elisei, L. Latterini, and U. Mazzucato.** 2002. Photophysical properties and antibacterial activity of meso-substituted cationic porphyrins. Photochem. Photobiol. **75:**462–470.
34. **Rex, J. H., M. G. Rinaldi, and M. A. Pfaller.** 1995. Resistance of *Candida* species to fluconazole. Antimicrob. Agents Chemother. **39:**1–8.
35. **Smijs, T. G., R. N. S. van der Haas, J. Lugtenburg, Y. Liu, R. L. P. de Jong, and H. J. Schuitmaker.** 2004. Photodynamic treatment of the dermatophyte Trichophyton rubrum and its microconidia with porphyrin photosensitizers. Photochem. Photobiol. **80:**197–202.
36. **Smijs, T. G. M., and H. J. Schuitmaker.** 2003. Photodynamic inactivation of the dermatophyte Trichophyton rubrum. Photochem. Photobiol. **77:**556–560.
37. **Soncin, M., C. Fabris, A. Busetti, D. Dei, D. Nistri, G. Roncucci, and G. Jori.** 2002. Approaches to selectivity in the Zn(II)-phthalocyanine-photosensitized inactivation of wild-type and antibiotic-resistant Staphylococcus aureus. Photochem. Photobiol. Sci. **1:**815–819.
38. **Stefan, C. J., and K. J. Blumer.** 1999. A syntaxin homolog encoded by VAM3 mediates down-regulation of a yeast G protein-coupled receptor. J. Biol. Chem. **274:**1835–1841.
39. **Stenstrom, A. G., J. Moan, G. Brunborg, and T. Eklund.** 1980. Photodynamic inactivation of yeast cells sensitized by hematoporphyrin. Photochem. Photobiol. **32:**349–352.
40. **Strakhovskaya, M. G., A. O. Shumarina, G. Y. Fraikin, and A. B. Rubin.** 1999. Endogenous porphyrin accumulation and photosensitization in the yeast Saccharomyces cerevisiae in the presence of 2,2′-dipyridyl. J. Photochem. Photobiol. **49:**18–22.
41. **Strakhovskaya, M. G., V. G. Zhukhovitskii, A. F. Mironov, A. M. Seregin, E. F. Stranadko, and A. B. Rubin.** 2002. Fungicidal activity of khlorin photosensitizers. Dokl. Biochem. Biophys. **384:**155–158.
42. **Vergeldt, F. J., R. B. M. Koehorst, A. Vanhoek, and T. J. Schaafsma.** 1995. Intramolecular interactions in the ground and excited-state of tetrakis(*N*-methylpyridyl)porphyrins. J. Physical Chem. **99:**4397–4405.
43. **Wohlfarth, C.** 1995. Permittivity (dielectric constant) of liquids, p. 159–209. *In* D. R. Lide and H. P. R. Frederikse (ed.), Handbook of chemistry and physics. CRC Press, Inc., Boca Raton, Fla.
44. **Zoladek, T., B. N. Nguyen, I. Jagiello, A. Graczyk, and J. Rytka.** 1997. Diamino acid derivatives of porphyrins penetrate into yeast cells, induce photodamage, but have no mutagenic effect. Photochem. Photobiol. **66:**253–259.